

Multi-Frequency Precise Point Positioning Using GPS and Galileo Data with Smoothed Ionospheric Corrections

Francesco Basile, Terry Moore, Chris Hill

Nottingham Geospatial Institute
University of Nottingham
Nottingham, UK
francesco.basile@nottingham.ac.uk

Gary McGraw, Andrew Johnson

Rockwell Collins

Abstract—The poor signal visibility and continuity associated with urban environments together with the slow convergence/re-convergence time of Precise Point Positioning (PPP), usually makes PPP unsuitable for land navigation in cities. However, results based on simulated open areas demonstrated that, once Galileo reaches final operational capability, PPP convergence time will be cut in a half using dual-constellation GPS/Galileo observations. Therefore, it might be possible to extend the applicability of PPP to land navigation in certain urban areas. Preliminary results, based on simulations, showed that GPS/Galileo PPP is possible where buildings are relatively short and satellites minimum visibility requirement is met for most of the time. In urban environments, signal discontinuity and re-convergence still represent the major problem for traditional PPP, which is based on the ionosphere-free combination of two-frequency pseudo-range and carrier phase. An alternative method to mitigate the ionosphere delay is proposed in order to ensure the best positioning performance from multi-frequency PPP. Instead of using the ionosphere-free combination, here low noise dual- or triple-frequency pseudo-range combinations are corrected with ionosphere delay information coming from federated carrier smoothing (Hatch) iono-estimation filters for each satellite. This method provides faster re-convergence time and ensures the best possible positioning performance from the Galileo Alternative BOC modulation in multi-frequency PPP. Indeed, even though Galileo E5 has small tracking noise and excellent multipath rejection, its PPP positioning performance is limited by the influence of E1 signal errors in the ionosphere-free combination, degrading the quality of the measurements.

Keywords—GPS; Galileo; Multi-Constellation; Multi-Frequency; PPP

I. INTRODUCTION

Precise Point Positioning (PPP) [1] is a carrier phase based positioning technique that enables centimeter-level (static processing) to decimeter-level (kinematic processing) accuracy, with no need for local reference stations as required

with Real Time Kinematic (RTK) techniques. PPP can be considered as an improved version of the classic pseudo-range based positioning [2], in which broadcast navigation data are replaced with precise orbits and clock estimates from a global or regional network solution. Models for environmental and site location effects are also required. Using carrier phase measurements, in addition to code pseudo-ranges, means that the initial carrier phase ambiguities have to be estimated, causing long convergence times. Typically, 15 to 60 minutes are required to have the final accuracy. This long convergence time represents a drawback of PPP and explains why PPP has not been widely used in constrained and transient signal environments associated with urban areas. Indeed, in case the GNSS receiver loses track of carrier phase, the positioning filter needs to be reinitialized, meaning that further tens of minutes are required before re-convergence.

With the advent of the new Global Navigation Satellite Systems (GNSSs), significant research efforts have been dedicated to study the navigation performance of multi-GNSS, both in terms of signal availability and positioning accuracy in multiple scenarios, including urban environments. In particular, it was demonstrated that, on major roads of cities, satellite availability is strongly improved when using at least two systems (e.g. GPS and Galileo) with respect to the GPS-only case [3, 4]. However, for very dense urban canyons multi-constellation GNSS fails to meet the minimum requirements for positioning, most of the time, even considering three systems together [3]. Analysis using both simulated [5, 6] and real data [7, 8] showed that, once Galileo reaches final operational status, the PPP convergence time will be cut by more than a half when using both GPS and Galileo observations. Therefore, multi-GNSS will open PPP to a wider range of applications.

This paper assesses the performance improvement offered by future operational-state dual-constellation (GPS and Galileo) compared to the single-constellation case, not only for

the environments for which PPP has traditionally been applied, namely open sky conditions, but also urban environments.

II. MULTI-CONSTELLATION MULTI-FREQUENCY GNSS SIMULATOR

Assessing final operational state multi-constellation GNSS performance with real data is hampered by the current incomplete deployment of the Galileo constellation and the lack of freely available, real-time, PPP precise orbit and clock products for modernized GNSS. Therefore a simulator for multi-GNSS observations and precise PPP orbit and clock products was developed in Simulink to support this research.

The simulator inputs consist of the reference trajectories for the user and the transmitting satellites and the information about the receiver and satellite clock offset and drift. The simulator outputs GNSS measurements in Receiver Independent Exchange (RINEX) 2.11 observation format.

Code pseudo-range $P_{u,k}^s$ and carrier phase $L_{u,k}^s$, transmitted on frequency k by satellite s , are simulated considering the main source of errors as described in [2].

$$P_{u,k}^s = r + c(dt_u - dt^s + \delta t^{\text{rel}}) + c(d_{u,k} + d_k^s) + I_{u,k}^s + T_u^s + \varepsilon_{P,u,k}^s \quad (1)$$

$$L_{u,k}^s = r + c(dt_u - dt^s + \delta t^{\text{rel}}) - I_{u,k}^s + T_u^s - \lambda_k N_{u,k}^s + \varepsilon_{L,u,k}^s \quad (2)$$

Equations (1) and (2) are the generic pseudo-range and carrier phase equations. They include: the geometric range r , the receiver and satellite clock offsets dt_u and dt^s , the relativistic effect δt^{rel} , the group delays for receiver ($d_{u,k}$) and satellite (d_k^s), the atmospheric delays due to ionosphere $I_{u,k}^s$ and troposphere T_u^s , the carrier phase initial ambiguity $N_{u,k}^s$, and other errors including pseudo-range and carrier phase noise and multipath ($\varepsilon_{P,u,k}^s$ and $\varepsilon_{L,u,k}^s$). Details of the models to simulate these errors can be found in [9].

Precise orbits and clocks are also required in PPP. Therefore, the simulator also outputs real-time quality precise products in Standard Products 3 (SP3) and RINEX clock 2.0 formats. The simulated products' error is based on the comparison between the GPS IGS real-time and ESA final products between GPS weeks 1917 and 1920.

As described in [9], the error in the real-time products Δ_{RT} can be modelled as the sum of two sinusoid with periods equal to the Earth rotation period T_E (23 hours and 56 minutes) and to the orbital period of the constellation T_O (11 hours and 58

minutes for GPS, while for Galileo it is 14 hours and 22 minutes).

$$\Delta_{\text{RT}} = b + a_E \sin\left(\frac{2\pi}{T_E} t + \Phi_E\right) + a_O \sin\left(\frac{2\pi}{T_O} t + \Phi_O\right) \quad (3)$$

The average biases b and amplitudes a_O and a_E for each component is summarized in Table I.

III. POSITIONING IN OPEN SKY CONDITIONS

Over the years, PPP has largely been applied to many real-time applications that require sub-decimeter level accuracy on a wide area or global scale. In precision farming, for instance, PPP can be used to precisely navigate field machines to fulfil the high accuracy requirements over areas of hundreds of square kilometers [10]. Also, precise positioning in offshore and desert areas cannot expect to have any nearby stations due to logistical feasibility and cost, therefore PPP can be used for ocean drilling, sea floor and sea surface mapping or tsunami monitoring. All these scenarios are characterized by open sky conditions, where a receiver is more likely to have continuous track of the GNSS satellites.

In this section, the positioning performance of GPS and Galileo signals, alone or used together, in open sky conditions will be assessed. To do this, simulated observations, 24 hours long, from ten static receivers spread worldwide (see Fig. 1) were processed with the POINT software [11] in static PPP mode with float ambiguity. For each station, the simulator was run 55 times; therefore a total of 550 points were considered.

TABLE I. RMS OF THE FITTING PARAMETERS. VALUES ARE IN UNITS OF CENTIMETERS.

	Radial	Along-track	Cross-track	Clocks
b	1.48	3.99	1.92	17.3
a_O	1.30	4.17	2.22	6.64
a_E	1.04	2.11	1.62	4.36



Fig. 1. Stations considered for the open sky test.

For better GPS-Galileo interoperability, PPP results based on the ionosphere free (IF) combination between GPS L1 and L5 and Galileo E1 and E5a were considered.

The metrics used to define the positioning performance are the errors in the north, east and down components of the position at the end of the processing and the time these errors take to converge below 10 centimeters.

The open sky condition always guarantees excellent geometry and signal continuity even considering only one constellation. For example, Fig. 2 shows the epochs of the day in which a given GNSS satellite is visible from station SEY2. Individual GPS satellites were continuously visible for up to 10 hours and 48 minutes, while Galileo satellites for maximum 14 hours and 18 minutes. This difference is due to the higher altitude of the Galileo orbits, and consequently lower velocity of the satellites, with respect to GPS. In terms of ambiguity resolution, having signals continuously available for a longer time is beneficial, but faster change in satellite geometry leads to better observability of the ambiguity itself. Fig. 3 shows the Position Dilution of Precision (PDOP) for the GPS only, Galileo only, and GPS plus Galileo cases as seen by station SEY2. Over 24 hours, on average the PDOP for the GPS only case is 9% smaller than the PDOP for the Galileo only case, while using two constellations the PDOP is further improved by 36% with respect to the Galileo case.

A. PPP results

Table II shows the root mean square (RMS) of the errors and convergence times in the three components of position for the different configurations for the 550 points considered. Both single and dual constellation systems are able to provide a sub-decimeter level accuracy after a few tens of minutes. On average, positioning with Galileo E1-E5a IF performs better than GPS L1-L5 IF: it is more accurate and converges faster than the GPS solution.

Approximately 80% of improvement was registered in the horizontal accuracy, while the vertical error improved by 11%. However this does not really matter as both systems can guarantee the target accuracy of better than 10 centimeters.

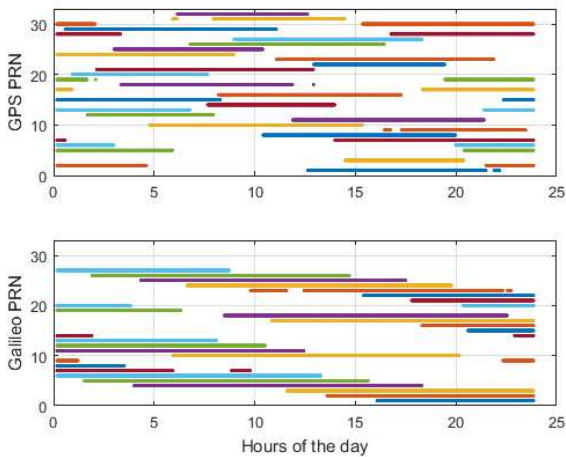


Fig. 2. Satellite availability as recorded by station SEY2.

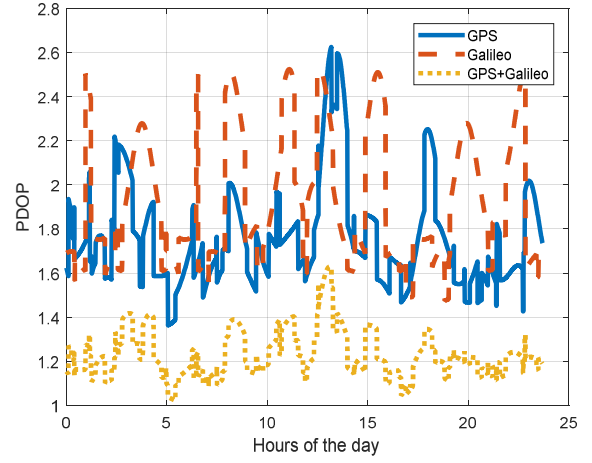


Fig. 3. PDOP daily time series as seen by station SEY2 for the single and two-constellation cases.

TABLE II. COMPARISON BETWEEN GPS-ONLY, GALILEO-ONLY AND GPS PLUS GALILEO PPP RESULTS. RMS OF THE POSITIONING ERRORS AND CONVERGENCE TIMES FOR THE STATIONS CONSIDERED.

	Errors [cm]		
	North	East	Down
GPS L1-L5	0.86	1.76	3.55
Galileo E1-E5a	0.16	0.36	3.15
GPS L1-L5 Galileo E1-E5a	0.42	1.00	3.24
Galileo E1-E5	0.16	0.37	3.15
	Convergence time [minutes]		
	North	East	Down
GPS L1-L5	17	37	56
Galileo E1-E5a	17	32	34
GPS L1-L5 Galileo E1-E5a	12	20	28
Galileo E1-E5	17	33	36

What is really relevant is the improvement in the convergence time. In the Galileo case, the vertical component converges 39% faster than the GPS case, while the horizontal components converge up to 13% faster.

As it was already highlighted in [9], the reason for this behavior is the lower noise on Galileo pseudo-ranges [12]. Further improvement in the convergence time were observed when using the two systems together. The time the vertical errors takes to go below 10 centimeters was reduced by 50% with respect to the GPS only case and by 18% with respect to the Galileo only case. The overall accuracy is half way between the one obtained by GPS PPP and Galileo PPP, but, as previously stated, this does not represent a major concern being well below the 10 centimeters threshold.

Having demonstrated that lower pseudo-range noise leads to better positioning performance, one would expect some improvements by employing the Galileo Alternative BOC

modulated signal E5. It is known to have small tracking noise and excellent multipath rejection. However, as shown in Table II, when comparing the PPP solutions obtained using the Galileo E1-E5 IF and E1-E5a IF combinations, they have nearly the same performance. The reason can be found in the influence of E1 signal errors in the IF combination, which degrade the quality of the measurements.

IV. POSITIONING IN URBAN ENVIRONMENTS

The poor signal visibility and continuity associated to urban environments together with the slow (re-) convergence time of PPP, usually make it unsuitable for land navigation in cities. However, as demonstrated in the previous section, using dual-constellation not only improves the visibility conditions but also reduces the PPP convergence time. Therefore, it might be possible to extend the applicability of PPP to land navigation in certain urban areas.

In order to assess the positioning performance of two-constellation GNSS in these constrained environments, the signal availability and geometry in six different simulated sites in the neighborhood of the University College of London (UCL) campus were analyzed. Building boundaries [13], i.e. the minimum elevation angle above which GNSS signals can be received due to building obstruction, were adopted. Fig. 4 and Fig. 5 illustrates the location and the building boundaries for each site.

Sites B, C and D are three examples of streets that might be travelled when navigating a ground vehicle in European cities. Site B (Gower Street) is a three lane street plus footpaths with relatively small buildings (four-five stories) on each side of the road. Site C (University Street) is slightly narrower than Gower Street. It has only one lane, plus parking slots and footpaths on each side. Site D (Huntley Street) is as large as University Street but it is surrounded by taller buildings (six-seven floors), which make this site to be the most challenging in terms of signal obstruction. Indeed the minimum elevation angle for signal visibility associated to site D can be as large as 79 degrees. Site E corresponds to the front yard of the Wilkins Building in the UCL campus. This building offers very little obstruction to satellite visibility. For sites A and F, three and four streets, respectively, form a junction.

Traditionally, in PPP using IF code and carrier measurements, the state vector includes the three components of the position, the receiver clock offset, the residual zenith wet tropospheric delay, and the carrier phase ambiguity. Therefore, the minimum number of satellite required for PPP is five. The geometry conditions are also an important factor to assess the GNSS positioning performance. For land navigation particularly relevant is the Horizontal Dilution of Precision (HDOP), which provides information about the horizontal accuracy achievable. For many land applications, such as

precision agriculture and urban positioning, horizontal accuracy is more critical than vertical accuracy. Assuming that the ranging error in the carrier phase is 20 cm, in order to have decimeter level horizontal accuracy, HDOP needs to be no larger than 5. In most cases HDOP as little as 2 are common.

Table III is an overview of the visibility and geometry conditions in these sites. A two-constellation (GPS and Galileo) receiver, placed at either site E or at the two junctions, will always, or almost, see at least five satellites with an HDOP better than 5. In the two streets surrounded by shorter buildings (site B and C), the minimum requirement for signal availability and geometry is met for more than 80% of the day. This percentage drops to about 43% (site B) and 17% (site C) if we want to have HDOP values better than 2. The obstruction given by high buildings, as in site D, allows to have decent geometry conditions for only less than 6% of the epochs.

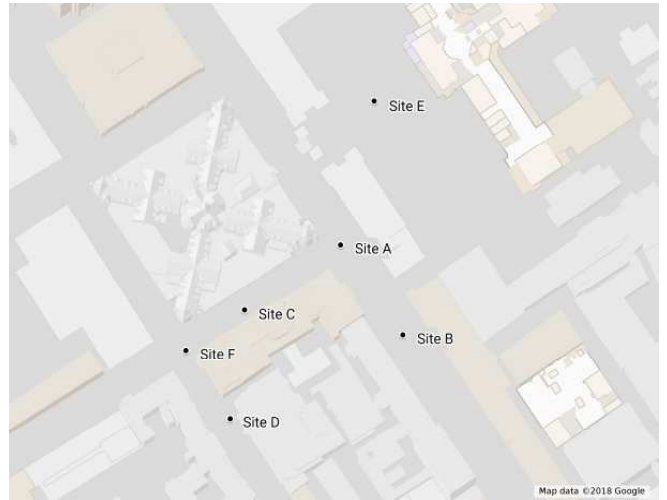


Fig. 4. Location of the urban sites that were considered in the analysis.

TABLE III. PERCENTAGE OF EPOCHS FOR WHICH TWO-CONSTELLATION GNSS MEETS THE MINIMUM VISIBILITY AND GEOMETRY REQUIREMENTS.

Site	$N \geq 5$	$N \geq 5 \text{ \& } HDOP \leq 5$	$N \geq 5 \text{ \& } HDOP \leq 2$
A	100%	100%	98.04%
B	97.24%	83.32%	43.18%
C	98.78%	81.54%	16.61%
D	36.03%	5.87%	0%
E	100%	100%	100%
F	100%	98.43%	70.52%

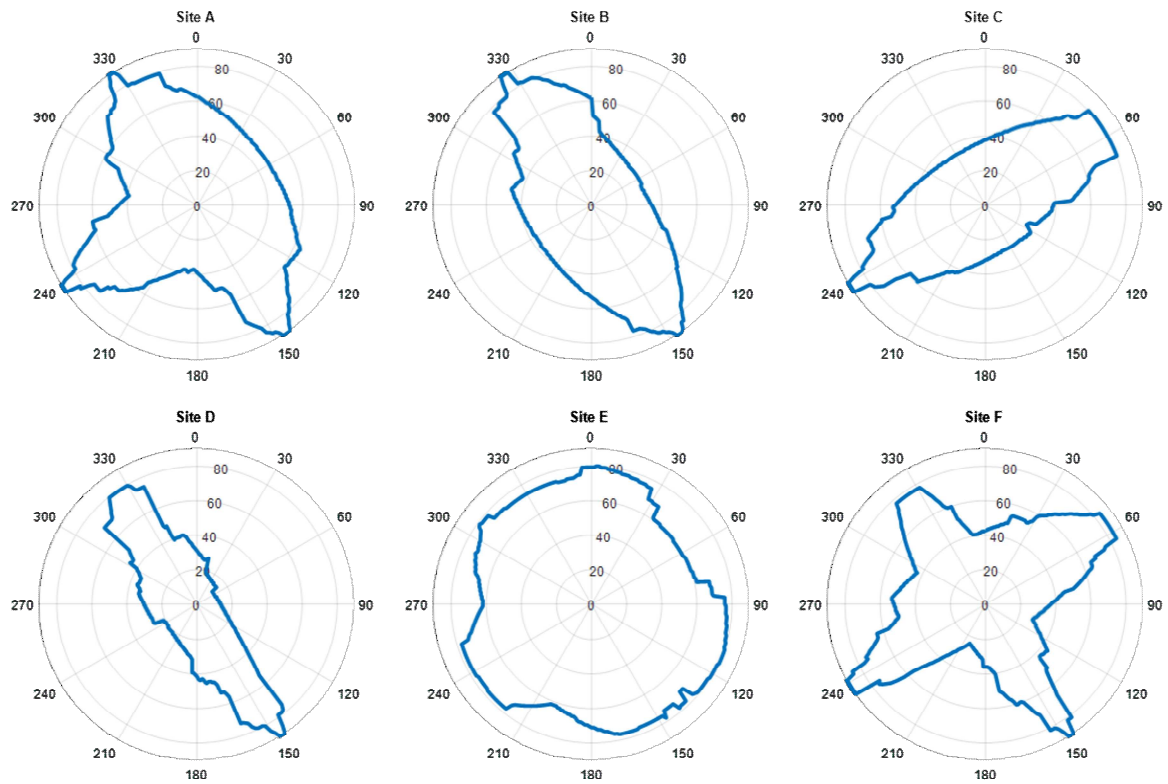


Fig. 5. Building obstruction masks to satellite visibility for each site.

From this preliminary study, it seems clear that high accuracy positioning in urban environments is possible, but only in some areas. Traditional European cities with narrow streets and six or more story buildings packed together aren't good candidates for PPP. PPP can in theory be performed in those urban areas where buildings are relatively short that provides good signal availability and geometry. However, it is well known that an additional obstacle of urban environments for PPP is signal discontinuity. Indeed, in case the GNSS receiver loses track of the carrier phase, the positioning filter needs to be reinitialized, meaning that further tens of minutes are required before re-convergence.

To test the re-convergence time of PPP in transient signal environments, a pedestrian carrying a multi-GNSS receiver is simulated to be walking along the path in Fig. 6. The receiver is supposed to be located for the first half hour of the simulation in the site E, before starting to move. This is to allow the initial convergence of the PPP filter.

Fig. 7 shows the visibility for a given GNSS satellite. Only the epochs when the receiver is moving are considered. Therefore, the first thirty minutes, when the receiver is static, are not included in the plot. Data gaps due to buildings obstruction are often visible. As a consequence, the carrier phase ambiguities need to be estimated all over again; this process usually requires tens of minutes before re-convergence.

Fig. 8 and 9 show the HDOP and the horizontal components of the position error for the kinematic test when GPS L1 and L5 and Galileo E1 and E5a, linearly combined

into the IF combination, are processed in kinematic PPP mode with the POINT software. It is possible to see how the horizontal error is at centimeter level when, at the beginning of the kinematic test, the HDOP is well below 5. 33 minutes after the beginning of the simulation, a few satellites go behind the buildings, they are out of sight and the HDOP rises to more than 30. At this point the errors are as large as 1.63 m. After the receiver has lost track of these satellites, the horizontal solution does not converge to centimeter level. However the errors go below 50 cm after four minutes. Towards the end of the simulation, the HDOP jumps to more than 90, with the east error increasing to about 24 m.



Fig. 6. Path for the kinematic PPP test in urban environment.

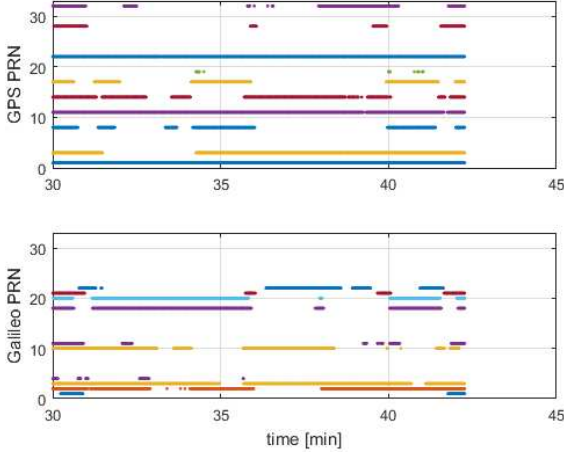


Fig. 7. Satellites availability during the kinematic test.

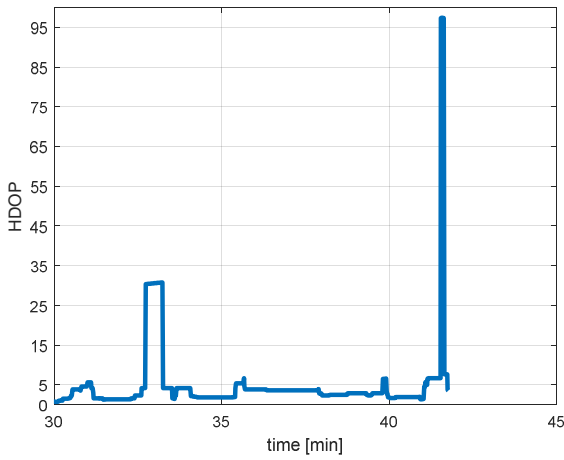


Fig. 8. HDOP for the kinematic test.

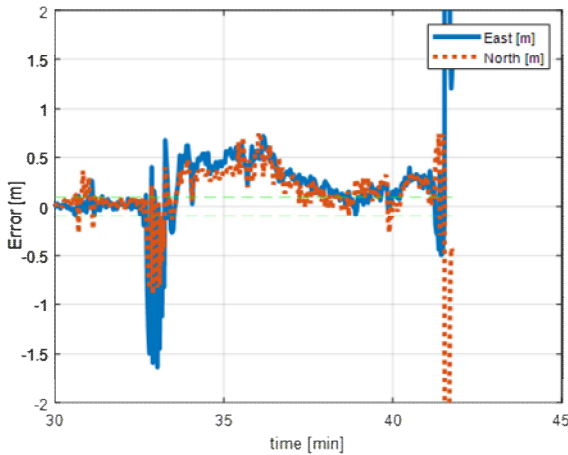


Fig. 9. Horizontal components of the positioning errors when L1-L5 IF and E1-E5a IF are processed in kinematic PPP mode for the simulated urban test in Fig. 6. The green dashed lines represent the 10 centimetres limit.

From this simulation test, it can be concluded that two-constellation PPP has in theory the potential to precisely navigate ground vehicles in some urban environments, however it is too sensitive to signals discontinuity. Solution re-convergence to decimeter-centimeter level still represents the main limitation to the use of PPP for high accuracy applications in cities. Nonetheless, GPS plus Galileo PPP easily enables sub-meter level horizontal accuracy for most of the simulation. After signal loss, it only took a few minutes to have a horizontal accuracy of better than a meter.

V. SMOOTHED IONOSPHERIC CORRECTION

Approaches for improving (re-) convergence of PPP include ambiguity fixing methods [14-16] based on the IF and wide-lane combinations and PPP algorithms in which the ionospheric delays are estimated in the state vector [17, 18]. Ambiguity fixing methods are immature and require extensions to monitoring network processing. The performance of ionospheric estimation depends on spatial and temporal constraints used for estimating the ionosphere in the PPP filter and on careful handling of the differential code biases (DCBs). These techniques yield performance improvements, particularly in the re-convergence time [19]. However, the computational penalty associated with the filter formulated with dual-frequency measurements and ionospheric states becomes more pronounced with increasing numbers of satellites associated with the use of multiple constellation, which is desirable for PPP in degraded signal environments.

As an alternative, [9] proposed a method to mitigate the ionosphere and intended to reduce the re-convergence time of the PPP solution, after initial convergence has been achieved. This is based on using a smoothed ionosphere correction proposed in [20] for local area differential processing. In this new approach, the ionospheric delay information, computed using the geometry-free combination of two-frequency pseudo-ranges, is smoothed by a Hatch filter before being applied to the pseudo-range, while the two-frequency carrier phases are linearly combined in the traditional IF combination.

$$\mathcal{I}_{i,j}^p = \begin{cases} I_{i,j}^p & , j=1 \\ \frac{1}{j} I_{i,j}^p + \left(1 - \frac{1}{j}\right) \left[\mathcal{I}_{i,j-1}^p + (I_{i,j}^L - I_{i,j-1}^L) \right] & , j < N \\ \frac{1}{N} I_{i,j}^p + \left(1 - \frac{1}{N}\right) \left[\mathcal{I}_{i,j-1}^p + (I_{i,j}^L - I_{i,j-1}^L) \right] & , j \geq N \end{cases} \quad (4)$$

$$I_1^p = \frac{P_1 - P_2}{1 - \frac{f_1^2}{f_2^2}} \quad (5)$$

$$I_1^L = -\frac{L_1 - L_2}{1 - \frac{f_1^2}{f_2^2}} \quad (6)$$

In this configuration, divergence does not represent a problem [21], since the opposite sign of the ionospheric term in the pseudo-ranges and phases is taken into account. Therefore, a smoothing window (N) even as large as the whole observation period can be selected, resulting in excellent smoothing with no divergence, as shown in Fig. 10.

Assuming the noise on pseudo-range P_k to be white with a standard deviation σ_k and that there is no correlation between the pseudo-ranges, the error in the smoothed ionosphere correction can be estimated as in

$$\sigma_{I_{ij}}^2 = \frac{1}{j^2} \sigma_{I_1}^2 + \left(1 - \frac{1}{j}\right)^2 \sigma_{I_{j-1}}^2 \quad (7)$$

$$\sigma_{I_1}^2 = \frac{\sigma_1^2 + \sigma_2^2}{1 - \frac{f_1^2}{f_2^2}} \quad (8)$$

$$\sigma_{I_{ij}}^2 = \sigma_{I_{j-1}}^2 + 2\sigma_{I_1}^2 - \left(1 - \frac{1}{j-1}\right) \sigma_{I_1}^2 \quad (9)$$

$$\sigma_{I_1^L}^2 = \frac{\sigma_{L_1}^2 + \sigma_{L_2}^2}{1 - \frac{f_1^2}{f_2^2}} \quad (10)$$

Once the Hatch filter has converged, ideally we have IF pseudo-ranges with lower noise than the traditional ones. Therefore, in transient signal environments associated with urban canyons and in case the PPP filter needs to restart, we can obtain a quicker re-convergence thanks to the lower noise on the ionosphere corrected pseudo-ranges. Indeed, provided that the signal gap is not very large, the ionosphere smoothing filter doesn't need to be restarted from the raw values. Since the change of rate of the ionospheric delay doesn't change that much from epoch to epoch, the old information about how the ionosphere changes with the time can be used to propagate even in case of cycle slips.

A. Low noise multi-frequency combinations

The results presented in [9] proved that the convergence time in PPP would be shorter if the noise on pseudo-ranges could be reduced. The method introduced in the previous section allows users to be free from the constraint of IF observables and, therefore, to look for multi-frequency combinations aimed to minimize the noise on the pseudo-

ranges. The next generation GNSS satellites will broadcast open signals over three frequencies. A linear combination P between the three pseudo-ranges P_1 , P_2 and P_3 can be written in a simplified form as in (11).

$$\begin{aligned} P &= \alpha_1 P_1 + \alpha_2 P_2 + \alpha_3 P_3 \\ &= (\alpha_1 + \alpha_2 + \alpha_3)g + \\ &\quad + \left(\alpha_1 + \alpha_2 \frac{f_1^2}{f_2^2} + \alpha_3 \frac{f_1^2}{f_3^2} \right) I_1 + \varepsilon_P \end{aligned} \quad (11)$$

Where g includes the geometric range, clocks and the troposphere terms, I_1 is the ionospheric delay on P_1 and ε_P is the noise on the combination, which has a standard deviation σ_P .

$$\begin{aligned} \sigma_P &= \sqrt{\alpha_1^2 \sigma_1^2 + \alpha_2^2 \sigma_2^2 + \alpha_3^2 \sigma_3^2} \\ &= \sigma_1 \sqrt{\alpha_1^2 + \alpha_2^2 n_2^2 + \alpha_3^2 n_3^2} \end{aligned} \quad (12)$$

We can define an ionosphere amplification factor q and a noise amplification factor n of the combination as

$$q = \left(\alpha_1 + \alpha_2 \frac{f_1^2}{f_2^2} + \alpha_3 \frac{f_1^2}{f_3^2} \right) = (\alpha_1 + \alpha_2 q_2 + \alpha_3 q_3) \quad (13)$$

$$n = \sqrt{\alpha_1^2 + \alpha_2^2 n_2^2 + \alpha_3^2 n_3^2} \quad (14)$$

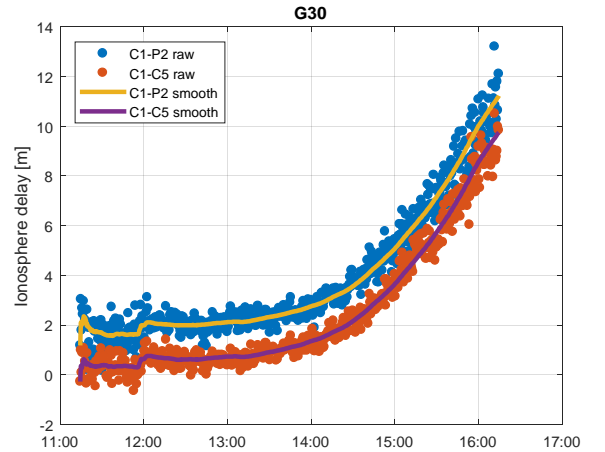


Fig. 10. Ionosphere delay computed from C1-P2 combination (raw blue dots, smoothed yellow line) and C1-C5 combination (raw orange dots, smoothed purple line). GPS PRN 30 observed from BOGT on the 6th September 2016. On that day, a minor solar storm made the ionosphere particularly active.

In order to preserve g in the combination, the following condition must be satisfied

$$\alpha_1 + \alpha_2 + \alpha_3 = 1 \quad (15)$$

Together (13), (14), and (15) describe a surface in the space q - α_3 - n . The combination that guarantees the minimum noise amplification factor can be used for positioning purposes. Table IV summarizes the assumed values for n_i . Fig. 11 shows a color map of the noise amplification factor associated with the geometry preserving combination between GPS L1, L2 and L5. The noise for this combination can be as little as 0.57 times the noise on L1, while the corresponding ionosphere amplification factor is 1.49. This noise amplification is 37% smaller than the one for L5, which is the least noisy GPS pseudo-range, and 77% less than the noise on the IF combination between L1 and L5. Therefore, we could potentially have even faster re-convergence if we apply the smoothed ionospheric correction to this combination rather than to the uncombined L5 pseudo-range.

Similar conclusions can be drawn by considering Galileo signals. Using E1, E5a and E5b we can obtain 53% less noise than E1 alone and 37% less noise than E5a or E5b alone. Triple frequencies combinations involving E5 don't bring as large improvements respect to using E5 alone. Indeed maximum 16% less noise can be registered when combining E1, E5a and E5 respect to the E5 uncombined case. Table V illustrates the minimum noise amplification factor for each triple-frequency combination and its ionosphere amplification factor.

The noise associated to the ionosphere corrected multi-frequency pseudo-range combination, $\sigma_{\bar{P}}$, depends both on the error in the pseudo-ranges and in the smoothed correction. The latter is as large as meter-level before converging to centimeter-level. For this reason, a proper weighting method, that considers the varying noise on the ionosphere correction, needs to be defined. The noise on the ionosphere corrected pseudo-range combination \bar{P} can be expressed as in (17), where σ_{i, \tilde{I}_i} represents the covariance between the pseudo-range P_i and the smoothed ionosphere information.

$$\bar{P} = \alpha_1 P_1 + \alpha_2 P_2 + \alpha_3 P_3 - q \tilde{I}_1 \quad (16)$$

$$\begin{aligned} \sigma_{\bar{P}}^2 = & \alpha_1^2 \sigma_1^2 + \alpha_2^2 \sigma_2^2 + \alpha_3^2 \sigma_3^2 + q^2 \sigma_{\tilde{I}_1}^2 - \\ & - 2\alpha_1 q \sigma_{1, \tilde{I}_1} - 2\alpha_2 q \sigma_{2, \tilde{I}_1} - 2\alpha_3 q \sigma_{3, \tilde{I}_1} \end{aligned} \quad (17)$$

Assuming that the ionosphere delay is computed from the geometry free combination between P_1 and P_2 , the covariance σ_{i, \tilde{I}_1} at epoch k are as in

TABLE IV. ASSUMED NOISE ON GPS AND GALILEO PSEUDO-RANGES AND THEIR IONOSPHERIC DELAY RESPECT TO L1/ E1.

	n_i	q
L2	1.1	1.65
L5	0.9	1.79
E5a	0.75	1.79
E5b	0.75	1.70
E5	0.25	1.75
E6	1	1.52

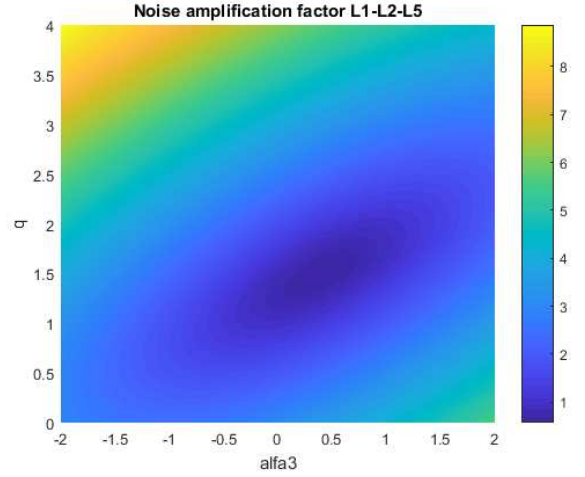


Fig. 11. Geometry preserving surface in the space q - α_3 - n for GPS L1-L2-L5 combinations.

$$\left. \begin{aligned} \sigma_{1, \tilde{I}_1} &= \frac{1}{1 - \frac{f_1^2}{f_2^2}} \sigma_1^2 \\ \sigma_{2, \tilde{I}_1} &= -\frac{1}{1 - \frac{f_1^2}{f_2^2}} \sigma_2^2 \\ \sigma_{3, \tilde{I}_1} &= 0 \end{aligned} \right\}, k=1 \quad (18)$$

$$\left. \begin{aligned} \sigma_{1, \tilde{I}_1} &= \frac{1}{1 - \frac{f_1^2}{f_2^2}} \frac{\sigma_1^2}{k} \\ \sigma_{2, \tilde{I}_1} &= -\frac{1}{1 - \frac{f_1^2}{f_2^2}} \frac{\sigma_2^2}{k} \\ \sigma_{3, \tilde{I}_1} &= 0 \end{aligned} \right\}, k > 1$$

To test the benefit of the new approach to the re-convergence time, three hours of simulated GPS and Galileo

data were processed with the POINT software in kinematic mode. After 90 minutes, the PPP filter was forced to restart to simulate re-convergence. The performance of the traditional L1-L5 IF combination were compared with those of single-frequency L1 and L5, as well as the triple-frequency pseudo-range combination, all corrected with the smoothed ionosphere delay coming from the Hatch filter. Fig. 12 shows the precision (3σ) of the horizontal components after filter restart. The new approach has much faster re-convergence than the traditional PPP based on the IF combination, particularly when the low noise triple-frequency combination is employed. Indeed, while the traditional method takes about 15 minutes to have an East error below 10 centimeters, using the low noise combination, this accuracy is achieved instantly. Good improvements are also visible when applying the approach to the uncombined pseudo-range. Similar conclusions might be drawn considering Galileo signals (Fig. 13). The E1-E5 IF combination requires more than 15 minutes for North convergence, while using E5 with the Hatch filter we have the horizontal solution converged straight away.

Also, the new method was tested with the kinematic simulation as in Section IV. Here, the GPS triple-frequency combined pseudo-range and Galileo E5 pseudo-range (both corrected with the smoothed ionosphere) are processed in kinematic PPP mode with the POINT software. Fig. 14 illustrates the North and East positioning errors. Two minutes after the receiver lost track of most of the satellites, the solution re-converged to centimeter-decimeter level and it took less than one minute to get below 50 cm.

VI. CONCLUSIONS

In this paper, a comparison between GPS-only, Galileo-only, and GPS plus Galileo PPP was performed. Results based on simulated open sky condition demonstrated that Galileo performs better than GPS thanks to an assumed lower E1-E5a IF noise with respect to L1-L5. Two-constellation PPP enables faster (re-)convergence as compared to the single constellation case.

An analysis on GNSS signals availability and continuity, and satellites geometry was also performed to study the feasibility of PPP in urban environments. Preliminary results, based on simulations, showed that dual-constellation (GPS plus Galileo) PPP is possible in urban areas with relatively short buildings in which the satellites availability minimum requirement is met for most of the time. However, signal discontinuity still represents the major problem for traditional PPP in urban environments, due to long re-convergence time.

Finally, a new PPP configuration based on triple-frequency combinations, intended to minimize the noise on the pseudo-range, and corrected by a smoothed ionospheric delay was proposed. This configuration seems to provide faster re-convergence than the traditional PPP with the IF combination.

TABLE V. MINIMUM NOISE ACHIEVABLE THROUGH GPS AND GALILEO TRIPLE-FREQUENCY PSEUDO-RANGE COMBINATIONS AND THEIR IONOSPHERIC DELAY RESPECT TO L1/ E1.

Combination	n_{\min}	$q(n_{\min})$
L1-L2-L5	0.57	1.49
E1-E5a-E5b	0.47	1.58
E1-E5a-E6	0.51	1.58
E1-E5b-E6	0.52	1.46
E1-E5a-E5	0.21	1.72
E1-E5b-E5	0.22	1.71
E1-E5-E6	0.22	1.70

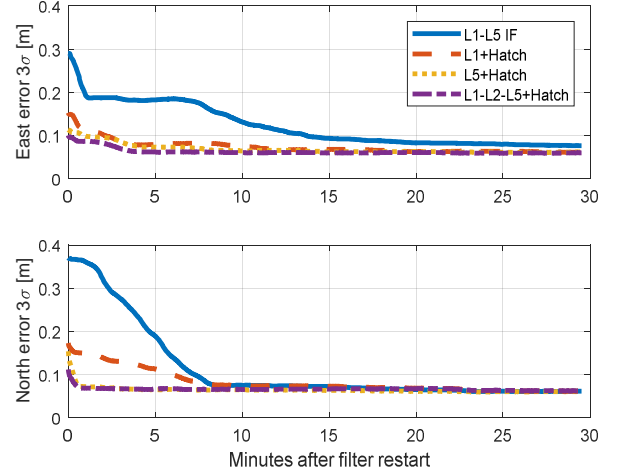


Fig. 12. Horizontal re-convergence comparison between traditional PPP based on GPS L1-L5 IF combination, single-frequency ionosphere corrected pseudo-range, and triple-frequency ionosphere corrected pseudo-range.

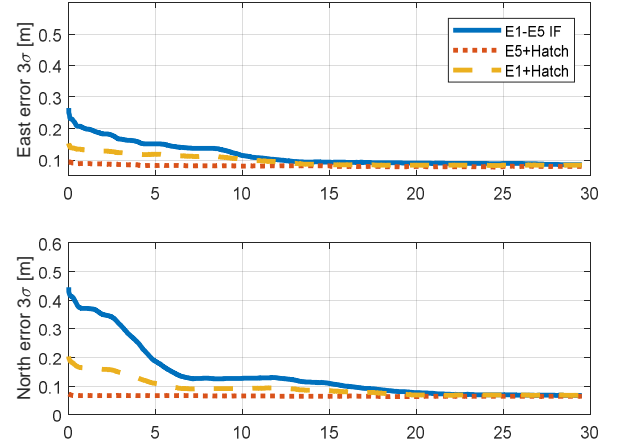


Fig. 13. Horizontal re-convergence comparison between traditional PPP based on Galileo E1-E5 IF combination and single-frequency ionosphere corrected pseudo-range.

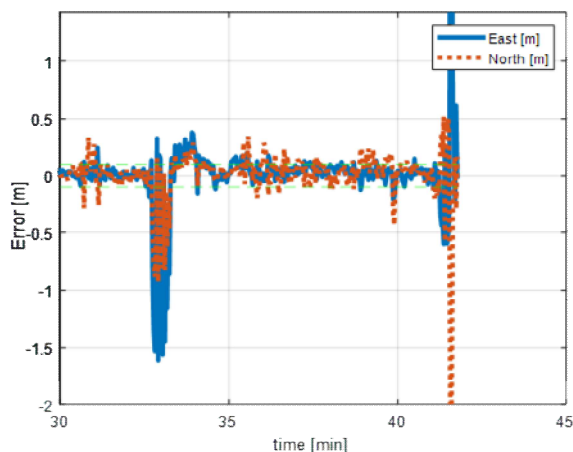


Fig. 14. Horizontal components of the positioning errors for the simulated urban test in Fig. 6 obtained with the new method. The green dashed lines represent the 10 centimetres limit.

ACKNOWLEDGMENTS

The authors wish to thank Dr. Paul Groves and Dr. Mounir Adjrad from UCL, and the Ordnance Survey for providing the building boundaries used in the simulations.

REFERENCES

- [1] J. F. Zumberge, M. B. Hefflin, D. C. Jefferson, M. M. Watkins, and F. H. Webb, "Precise point positioning for the efficient and robust analysis of GPS data from large networks," *Journal of Geophysical Research: Solid Earth*, vol. 102, pp. 5005-5017, 1997.
- [2] P. J. G. Teunissen and O. Montenbruck, *Springer Handbook of Global Navigation Satellite Systems*: Springer International Publishing, 2017.
- [3] S. Ji, W. Chen, X. Ding, Y. Chen, C. Zhao, and C. Hu, "Potential Benefits of GPS/GLONASS/GALILEO Integration in an Urban Canyon – Hong Kong," *Journal of Navigation*, vol. 63, pp. 681-693, 2010.
- [4] K. O'Keefe, "Availability and Reliability Advantages of GPS/Galileo Integration," in *ION GPS*, Salt Lake City, UT, 2001.
- [5] J. M. Juan, M. Hernandez-Pajares, J. Sanz, P. Ramos-Bosch, A. Aragon-Angel, R. Orus, *et al.*, "Enhanced Precise Point Positioning for GNSS Users," *IEEE Transactions on Geoscience and Remote Sensing*, vol. 50, pp. 4213-4222, 2012.
- [6] X. Shen and Y. Gao, "Analyzing the Impacts of Galileo and Modernized GPS on Precise Point Positioning," in *National Meeting of the Institute of Navigation*, Monterey, CA, USA, 2006, pp. 837-846.
- [7] J. Miguez, J. V. P. Gisbert, R. O. Perez, J. A. Garcia-Molina, X. Serena, F. Gonzales, *et al.*, "Multi-GNSS PPP Performance Assessment with Different Ranging Accuracies in Challenging Scenarios," in *International Technical Meeting of The Satellite Division of the Institute of Navigation*, Portland, OR, USA, 2016, pp. 2069-2081.
- [8] A. Afifi and A. El-Rabbany, "Performance Analysis of Several GPS/Galileo Precise Point Positioning Models," *Sensors (Basel)*, vol. 15, pp. 14701-26, 2015.
- [9] F. Basile, T. Moore, and C. Hill, "Analysis on the Potential Performance of GPS and Galileo Precise Point Positioning using simulated Real-Time products," in *International Navigation Conference (INC)*, 2017.
- [10] P. Mondal and V. K. Tewari, "Present Status of Precision Farming: A Review," *International Journal of Agricultural Research*, vol. 2, pp. 1-10, 2007.

- [11] A. Jokinen, S. Feng, W. Ochieng, C. Hide, T. Moore, and C. Hill, "Fixed ambiguity Precise Point Positioning (PPP) with FDE RAIM," presented at the ION PLANS, Myrtle Beach, SC, 2012.
- [12] T. Richardson, C. Hill, and T. Moore, "Analysis of Multi-Constellation GNSS Signal Quality," in *International Technical Meeting of The Institute of Navigation*, Monterey, CA, USA, 2016, pp. 631-638.
- [13] L. Wang, P. D. Groves, and M. K. Ziebart, "Multi-Constellation GNSS Performance Evaluation for Urban Canyons Using Large Virtual Reality City Models," *Journal of Navigation*, vol. 65, pp. 459-476, 2012.
- [14] P. Collins, S. Bisnath, F. Lahaye, and P. HÉRoux, "Undifferenced GPS Ambiguity Resolution Using the Decoupled Clock Model and Ambiguity Datum Fixing," *Navigation*, vol. 57, pp. 123-135, 2010.
- [15] D. Laurichesse, F. Mercier, J.-P. Berthias, P. Broca, and L. Cerri, "Integer Ambiguity Resolution on Undifferenced GPS Phase Measurements and Its Application to PPP and Satellite Precise Orbit Determination," *Navigation*, vol. 56, pp. 135-149, 2009.
- [16] M. Ge, G. Gendt, M. Rothacher, C. Shi, and J. Liu, "Resolution of GPS carrier-phase ambiguities in Precise Point Positioning (PPP) with daily observations," *Journal of Geodesy*, vol. 82, pp. 389-399, 2008.
- [17] X. Li, M. Ge, H. Zhang, and J. Wickert, "A method for improving uncalibrated phase delay estimation and ambiguity-fixing in real-time precise point positioning," *Journal of Geodesy*, vol. 87, pp. 405-416, 2013.
- [18] H. Zhang, Z. Gao, M. Ge, X. Niu, L. Huang, R. Tu, *et al.*, "On the convergence of ionospheric constrained precise point positioning (IC-PPP) based on undifferential uncombined raw GNSS observations," *Sensors (Basel)*, vol. 13, pp. 15708-25, Nov 18 2013.
- [19] X. Li, "Improving Real-time PPP Ambiguity Resolution with Ionospheric Characteristic Consideration," in *International Technical Meeting of The Satellite Division of the Institute of Navigation (ION GNSS)*, Nashville, TN, USA, 2012, pp. 3027 - 3037.
- [20] P. Y. Hwang, G. A. McGraw, and J. R. Bader, "Enhanced Differential GPS Carrier-Smoothed Code Processing Using Dual-Frequency Measurements," *Navigation*, vol. 46, pp. 127-137, 1999.
- [21] G. McGraw, B. A. Schnaufer, P. Y. Hwang, and M. J. Armatys, "Assessment of Alternative Positioning Solution Architectures for Dual Frequency Multi-Constellation GNSS/SBAS," in *International Technical Meeting of The Satellite Division of the Institute of Navigation*, Nashville, TN, USA, 2013, pp. 223-232.